# LIPOCALIN 2: A NEW MECHANORESPONDING GENE REGULATING BONE HOMEOSTASIS

Nadia Rucci[1*], PhD, Mattia Capulli[1*], PhD, Sara Gemini Piperni[1], MSc, Alfredo Cappariello[2], PhD, Patrick Lau[3], PhD, Petra Frings-Meuthen[3], PhD, Martina Heer[4], PhD, Anna Teti[1], PhD.

[1]Department of Biotechnological and Applied Clinical Sciences, University of L'Aquila, L'Aquila, Italy; [2]Bambino Gesù Children Hospital, "Istituto di Ricovero e Cura a Carattere Scientifico" (IRCCS), Rome, Italy; [3]German Aerospace Center (DLR), Institute of Aerospace Medicine, Cologne, Germany; [4]Department of Nutrition and Food Science, Nutritional Physiology, University of Bonn, Germany

*Equal contributors

**Running title:** Lipocalin 2 and mechanical unloading

**Keywords:** LCN2, adipokine, mechanical forces, unloading, osteoclasts, osteoblasts

**Corresponding Author:**

Anna Teti, Ph.D.
Department of Biotechnological and
Applied Clinical Sciences
Via Vetoio – Coppito 2
67100 L'Aquila, Italy
Tel. +39 0862 433511/13
Fax +39 0862 433523
E-mail: teti@univaq.it

**Grants:** This work was supported by the STRODER-SIOMMMS grant to NR, by a grant from the "Agenzia Spaziale Italiana" (ASI) to AT and by the DLR Space Programme to MH.

**Conflict of interest statement:** All the authors state that there are no conflicts of interest to disclose.

**ABSTRACT**

Mechanical loading represents a crucial factor in the regulation of skeletal homeostasis. Its reduction causes loss of bone mass, eventually leading to osteoporosis. In a previous global transcriptome analysis performed in mouse calvarial osteoblasts subjected to simulated microgravity, the most up-regulated gene compared to unit gravity condition was *Lcn2*, encoding the adipokine Lipocalin 2 (LCN2), whose function in bone metabolism is poorly known. To investigate the mechanoresponding properties of LCN2, we evaluated LCN2 levels in sera of healthy volunteers subjected to bed rest, and found a significant time-dependent increase of this adipokine compared to time 0. We then evaluated the *in vivo* LCN2 regulation in mice subjected to experimentally-induced mechanical unloading by i) tail suspension, ii) muscle paralysis by botulin toxin A (Botox) or iii) genetically-induced muscular dystrophy (MDX mice), and observed that *Lcn2* expression was up-regulated in the long bones of all of them, while physical exercise counteracted this increase. Mechanistically, in primary osteoblasts transfected with LCN2-expression-vector (OBs-Lcn2) we observed that *Runx2* and its downstream genes *Osterix* and *Alp* were transcriptionally down-regulated, and ALP activity was less prominent *versus* empty-vector transduced osteoblasts (OBs-empty). OBs-Lcn2 also exhibited an increase of the *Rankl/Opg* ratio and *IL-6* mRNA, suggesting that LCN2 could link osteoblast poor differentiation to enhanced osteoclast stimulation. In fact, incubation of purified mouse bone marrow mononuclear cells with conditioned media from OBs-Lcn2 cultures, or their co-culture with OBs-Lcn2, improved osteoclastogenesis compared to OBs-empty, while treatment with LCN2 had no effect. In conclusion, our data indicate that LCN2 is a novel osteoblast mechanoresponding gene and that its regulation could be central to the pathological response of the bone tissue to low mechanical forces.

## INTRODUCTION

Lipocalin 2 (LCN2), also known as 24p3 and Neutrophil Gelatinase-Associated Lipocalin (NGAL)[1,2], is a 25-kD adipokine belonging to a large superfamily of proteins that bind and transport lipids and other hydrophobic molecules. Consistent with its expression in several cell types and organs, including neutrophils, adipocytes, macrophages, liver and kidney, LCN2 is implicated in diverse functions. For instance, it takes part in the host innate immune response through its bacteriostatic effect induced by the binding of bacterial enterobactin siderophores, which limits bacterial iron acquisition[3]. Accordingly, LCN2 deficient mice are more sensitive to certain Gram-negative bacteria and die more readily of sepsis compared to wild type mice[4,5].

Recently, it has been demonstrated a role of LCN2 also in the energy metabolism. Indeed, this protein is highly expressed in the adipose tissue and circulating LCN2 levels are increased in obese animals and in patients with type 2 diabetes[6,7]. Moreover, serum concentrations of LCN2 are positively associated with waist circumference, percent of body fat, systolic blood pressure, fasting glucose and insulin concentrations, fasting triglycerides and markers of chronic inflammation[6]. Serum LCN2 levels are also elevated in patients with coronary heart disease and are associated with atherosclerosis[8]. Furthermore, the expression of LCN2 rises 1000-fold in humans and rodents in response to renal tubular injury, and it appears so rapidly in urine and serum that it is proposed to be an early biomarker of renal failure[9].

So far, two LCN2 cell surface receptors have been identified. One receptor, called 24p3R (alluding to LCN2's original name, 24p3), is a protein that originally was referred to as brain organic cation transporter, which is a membrane-associated protein with 12 predicted transmembrane helices[10]. A second LCN2 receptor is the well-characterized multiprotein receptor megalin-cubulin[11], expressed by kidney proximal tubule cells, which are known target cells of LCN2[12].

Despite the several recognized functions accomplished by LCN2 in different tissues under physiologic and pathologic conditions, there are many questions still unsolved about the role of this molecule in the body. Since the function of LCN2 in bone homeostasis is barely known, we sought to investigate its involvement in this context based on a previous work in which we demonstrated that LCN2 could be a mechanoresponding gene that correlated with poor osteoblast activity[13]. In fact, in a global transcriptome analysis of mouse calvarial osteoblasts grown for 5 days under modeled microgravity (0.08*g* and 0.008*g*) to simulate low mechanical loading, we evidenced modulation of transcripts involved in osteoblast differentiation, as well as changes in the expression of a set of genes not previously correlated with bone metabolism, among which the most up-regulated gene was *Lcn2*[13].

Based on this evidence, the aim of this study was to in-depth investigate the role of LCN2 in the response of bone to mechanical unloading *in vivo* and *in vitro*. We demonstrated that LCN2 is up-regulated in human and animal models of reduced mechanical forces, and identified the cellular mechanisms underlying its effects on osteoblasts and osteoclasts.

## MATERIALS AND METHODS

### *Materials*

DMEM (Dulbecco's modified Minimum Essential Medium), FBS (Fetal Bovine Serum), penicillin, streptomycin and trypsin were from GIBCO (Uxbridge, UK). Sterile plastic ware was from Falcon Becton-Dickinson (Cowley, Oxford, UK) or Costar (Cambridge, MA, USA). Trizol reagent, primers and reagents for RT-PCR were from Invitrogen (Carlsbad, CA). The Brilliant® SYBR® Green QPCR master mix was from Stratagene (La Jolla, CA). Human recombinant (hr) Receptor Activator of Nuclear Factor κ-light-chain-enhancer of activated B cells transcription factor Ligand (RANKL) (#310-01) and hrMacrophage-Colony Stimulating Factor (M-CSF) (#300-25) were from Peprotech (EC, London). Anti-megalin antibody (cat.#sc-16478) was from Santa Cruz Biotechnology, Inc. (Santa Cruz, CA); anti-LCN2 antibody (cat.# AF1857), mouse recombinant (mr) Lipocalin2 (cat.# 1857-LC-050) and human ELISA kit for LCN2 (DLCN20) were purchased from R&D Systems Inc. (Minneapolis, MN). All the other reagents were of the purest grade from Sigma Aldrich Co. (St. Louis, MO, USA).

### *Ethics*

Approval for the study was obtained from the Ethical Committee of the "Aerztekammer Nordrhein", Düsseldorf, Germany, and was conducted in accordance with the latest version of the Declaration of Helsinki. The study is registered on http://www.clinicaltrials.gov with the unique trial number: NCT01183299 and registration date: 08/13/2010.

### *Protocol for the human study*

Primary focus of this bed rest study was to test if low-grade metabolic acidosis induced by high NaCl intake exacerbates bone resorption during immobilisation. For this reason, a 14-day head-down tilt bed rest (HDBR) study, including 8 male test subjects [mean age: 26.3 ± 3.5 years; body

weight (BW) 78.0 ± 4.3 kg] was conducted in the metabolic ward of the German Aerospace Center. Immobilization was accomplished with 6 degree HDBR, a valid ground-based model to simulate microgravity-induced bone loss[14]. During the bed rest period the subjects received in a cross-over design either a high (7.7 mEq /kg BW per day) or a low (0.7 mEq /kg BW per day) NaCl diet. The two parts of the study were performed separately with a 6-month washout period in between. Study design and primary outcome are described more detailed in Frings-Meuthen et al[14]. For the assessment of serum LCN2 levels in the present study, we took advantage of unutilized study samples.

***Blood sampling and analysis***

Blood samples were drawn on day 0 just before confinement to bed and during bed rest on days 4, 6, 8, 11 and 15. Blood samples were obtained by venipuncture from a forearm vein and collected into 5-ml serum separator tubes. After centrifugation, serum samples were aliquoted into 1ml cryotubes and kept frozen at −80 °C until use. LCN2 concentration was measured using a commercially available ELISA kit according to the manufacturer's recommendations.

***Animals***

Procedures involving animals care were conducted in conformity with national and international laws and policies (EEC Council Directive 86/609, OJ L 358, 1, Dec. 12, 1987; Italian Legislative Decree 116/92, *Gazzetta Ufficiale della Repubblica Italiana* n. 40, Feb. 18, 1992; NIH guide for the Care and Use of Laboratory Animals, NIH Publication No. 85-23, 1985), and were approved by the Institutional Review Board of the University of L'Aquila. At the end of the experiments, mice were sacrificed by $CO_2$ inhalation. All experiments were performed in female mice. Key experiments repeated in male mice showed similar results (not shown).

***Hindlimb suspension***

Hindlimb suspension was obtained according to Sakata et al.[15] on 8 week-old C57BL/6 mice. A strip of elastic tape forming half a circle at the center of the tail was applied to the ventral surface of the tail. A swivel attached to the half circle of tape was fixed to an overhead wire, the height of which was adjusted to maintain the mice suspended at an approximately 30° angle. The swivel apparatus allowed animals to readily access to food and water and to move freely into the cage using their forelimbs. After 21 days of suspension mice were sacrificed by $CO_2$ inhalation, hindlimbs were removed and cleaned from soft tissues, then they were frozen in dry ice and subjected to RNA extraction. An equal number of mice was maintained under normal cage conditions for 21 days as control.

***In vivo treatment with botulin toxin A (Botox)***

Eight week-old C57BL/6 mice were subjected to Botox injection according to Warner et al.[16]. Briefly, mice were anesthetized, then the left and the right hindlimbs of each mice were injected with saline solution (20 µl) and with Botox (2.0 unit/100gr), respectively, into the right quadriceps and the posterior compartment of the right calf (targeting gastrocnemius, plantaris, and soleus). The behavioral response of each mouse was quantified on days 1, 3, 7 and weekly thereafter using whole body weight measurement and assessment of gait disability. After 21 days mice were sacrificed, then the hindlimbs were removed, femurs and tibias were cleaned free of soft tissues and frozen in dry ice or fixed in 4% buffered paraformaldehyde for RNA extraction and morphometric analysis of bone parameters, respectively.

***MDX mice***

Eight week-old MDX (X chromosome-linked muscular dystrophy) homozygous mice (CB6F1/C57BL6 background) carrying a spontaneous single-base mutation on exon 23 of the

*dystrophin* gene[17,18] were used for analysis of the bone phenotype and for mRNA expression of LCN2 in tibias. Age-matched normal mice of the same background were employed as controls. Mice were euthanized by $CO_2$ inhalation, and hindlimb bones were excised, cleaned of soft tissues, frozen in dry ice and processed for RNA extraction.

***Treadmill exercise***

Wild-type (WT) and MDX mice were enforced to run on a mobile platform at a speed of 9 m/min for 30 min, twice a week for 3 weeks. Since mice carried muscular dystrophy, to avoid excessive stress due to increasing running time, physical exercise was not progressive.

***Forced swimming test***

WT mice subjected to hindlimb suspension were forced to swim in a 250 L water-filled tank (water depth=20 cm), with water temperature kept at 31°C. This test lasted 5 min and was repeated 3 times/day for 3 days/week during the entire period of unloading (3 weeks)[19]. Control mice were left for the same time of swimming test under unloading conditions.

***Micro Computed Tomography (μCT) analysis***

Tibias were mounted and acquired in a SkyScan 1174 with a voxel size of 6 μm (X-ray voltage 50 kV). Image reconstruction was carried out employing a modified Feldkamp algorithm using the Skyscan Nrecon software. Beam hardening correction and Fourier transform based ring artifact reduction were applied to the reconstructed images. ThreeD and 2D morphometric parameters were calculated for the trabecular bone of selected regions of interest, 150 slides 400 μm from the growth plate. Threshold values were applied for segmenting trabecular bone corresponding to bone mineral density values of 0.6/$cm^3$ calcium hydroxyapatite. ThreeD parameters were based on analysis of a Marching Cubes type model with a rendered surface[20]. Calculation of 2D areas and perimeters was

based on the Pratt algorithm. Bone structural variables and nomenclature were those suggested in Bouxsein et al.[21].

***Bone histomorphometry***

Tibias fixed in 4% paraformaldehyde were dehydrated in acetone and processed for glycol–methacrylate embedding without decalcification. Histomorphometric measurements were carried out on 5 μm–thick sections with an interactive image analysis system (IAS 2000; Delta Sistemi, Rome, Italy)[22] and with the suggested nomenclature[23]. Osteoclast surface/bone surface (%) was evaluated after histochemically staining the sections for TRAcP activity. Osteoblast surface/bone surface (%) was evaluated after staining the sections with methylene blue/azure II.

***Bone biomechanical properties***

Explanted femurs were cleaned out of soft tissues and stored at -80°C. They were then thawed in ice and soaked in ice-cold PBS. The analysis was performed on the distal portion of the femur using the Reference Point Indentation (Biodent Hfc, Active Life Scientific, Santa Barbara, CA). Samples were tested using the test probe BP2 and the following parameters: 10 indentation cycles at 2 Hz to a force of 4 N. Bones were maintained in an hydrated state throughout the test. Total indentation distance and total energy dissipation were calculated for each test. Five tests from each animal were averaged to produce a single value for each variable.

***Calvarial osteoblast cultures***

Calvariae from 7 day-old CD1 mice were removed, cleaned free of soft tissues and digested three times with 1 mg/ml *Clostridium histolyticum* type IV collagenase and 0.25% trypsin, for 20 min at 37°C with gentle agitation. Cells from the second and third digestions were plated and grown in standard conditions, in DMEM plus 10% FBS. At confluence, cells were trypsinized by standard

procedures and plated according to the experimental protocol. These cells expressed the osteoblast markers ALP, Runx-2, parathyroid hormone (PTH)/PTH related peptide receptor, type I collagen, and osteocalcin.

***Alkaline Phosphatase (ALP) activity assay***

Primary mouse osteoblasts were fixed in 4% paraformaldehyde for 15 min, then washed with PBS. ALP activity was evaluated histochemically using the Sigma-Aldrich kit n. 85, according to the manufacturer's instruction. Quantitative analysis was performed by scanning densitometry using the Molecular Analyst software for the model 670 scanning densitometer (Bio-Rad Laboratories) to obtain arbitrary density units.

***Amaxa nucleofector transfection***

One x$10^6$ primary mouse osteoblasts were nucleofected with 2 μg of empty- or LCN2-carrying pCMV-3TAG8 vectors, using the Amaxa Mouse Neuron Nucleofector kit (Lonza Cat. VPG-1001) and the program X-010 of the nucleofector device. After 48 hours from nucleofection, osteoblasts were employed for the experiments.

***Osteoclast primary cultures***

Bone marrow flushed out from the bone cavity of the long bones of 7 day-old CD1 mice was diluted 1:1 in Hank's balanced salt solution, layered over Histopaque 1077 solution and centrifuged at 400 *g* for 30 minutes. Cells were washed twice with Hank's solution, re-suspended in DMEM and plated in culture dishes at a density of $10^6$ cells/cm$^2$. After 3 hours, cell cultures were rinsed to remove non-adherent cells and maintained for 7 days in the same medium supplemented with 50 ng/ml rhM-CSF and suboptimal concentrations of rhRANKL (30 ng/ml), plus 100 ng/ml rmLCN2 or undiluted conditioned media from osteoblasts overexpressing LCN2 or transfected with an empty

vector as control.

***Osteoblast-osteoclast co-cultures***

Primary mouse osteoblasts, transfected by the AMAXA method with the LCN2 vector or with an empty vector, were plated in 48 well plates. When cells reached 30% confluence, purified mouse bone marrow mononuclear cells, obtained by the above described protocol, were added to the osteoblast cultures at a density of $10^6$ cells/ml. After 7 days of co-culture, osteoclasts were detected by Tartrate-Resistant Acid Phosphatase (TRAcP) histochemical staining.

***TRAcP activity assay***

Cells were fixed in 4% paraformaldehyde for 15 min, then extensively washed with the same buffer. TRAcP activity was detected histochemically, using the Sigma-Aldrich kit # 386, according to the manufacturer's instruction.

***Immunoisthochemistry***

Tibias were cleaned free of soft tissues and fixed with 4% paraformaldehyde for 48 hours, then decalcified in Osteodec for further 48 hours and embedded in paraffin to obtain 5µm thick sections. Sections were then deparaffinized, incubated with 0.07 M citrate buffer (pH 6) for 15 minutes at 98 °C for antigen retrieval, treated with 3% $H_2O_2$, and incubated overnight at 4 °C with the anti-Lcn2 mouse monoclonal antibody. The staining signal was revealed using the Dako LSAB System-HRP (cat# K0679, Dako North America, Inc., Carpinteria, CA, USA) following the manufacturer's instructions. Negative controls (omitting the primary antibody) were performed in parallel.

***Immunofluorescence***

Mouse primary osteoblasts were fixed with 4% paraformaldehyde and incubated for 1 h at room temperature with specific primary antibodies followed by FITC- or TRITC-conjugated secondary antibody. To detect nuclei, cells were stained with DAPI. Cells were then observed at room temperature by conventional epifluorescence (Axioplan; Carl Zeiss, Inc.) confocal (FluoView IX81 FVBF; Olympus) microscope. For fluorescence microscopy, we used 2.5× NA 0.075, 10× NA 0.30, 20× NA 0.5, and 40× NA 0.75 Plan-Neofluar objective lenses. Images were captured with a camera (AxioCam MRC5; Carl Zeiss, Inc.) using the AxioVs 40 version 4.7.1.0 software (Carl Zeiss, Inc.). For confocal microscopy, we used 10× NA 0.30 and 40× NA 0.85 UPlan-Apochromat or 60× NA 1.4 oil Plan-Apochromat objective lenses. Images were captured using FluoView 500 software (Olympus).

***Human Embryonic Kidney (HEK)293 cells***

The HEK293 cell line was obtained from the American Tissue Culture Collection (ATCC, Rockville, MD), and grown in DMEM supplemented with 10% FBS, 100 IU/ml penicillin, 100 µg/ml streptomycin, and 2 mM L-glutamine. Cells were grown in a 5% $CO_2$ humidified atmosphere at 37°C.

To overexpress LCN2, HEK293 cells were transiently transfected with the pCMV-3TAG8 expression vector containing LCN2, using the lipofectamine and PLUS reagent. Control transfectants were obtained by transfecting HEK293 cells with an empty pCMV-3TAG8.

***Semi quantitative and comparative real time RT-PCR***

Total RNA was extracted from mouse whole femurs or from osteoblasts using the Trizol®

procedure. RNA (1 μg) was reverse transcribed in cDNA using M-MLV reverse transcriptase and the equivalent of 0.1 μg was employed for the real time PCR reactions using the Brilliant® SYBR® Green QPCR master mix or for semiquantitative PCR. PCR conditions and primer pairs are listed in Table 1. Results, expressed as fold increase for real time RT-PCR, or shown by electrophoresis of PCR products in a 2% agarose gel plus ethidium bromide for conventional RT-PCR, were normalized *versus* the housekeeping gene *Gapdh*.

***Statistics***

Results are expressed as the mean ± SD of at least three independent experiments, 8 human subjects and at least 3 mice/group. Statistical analyses were performed by the Student's *t* test, the linear regression test or the non-parametric Mann–Whitney Runk Sum Test, according to the type of data sets. Statistical method is indicated in the figure legends. A p value $<0.05$ was conventionally considered statistically significant.

## RESULTS

### LCN2 expression in sera of patients subjected to prolonged bed rest

In our previous study we demonstrated that *Lcn2* is a mechanoresponding gene, up-regulated in mouse primary osteoblasts by mechanical unloading simulated in the NASA-developed rotating wall vessel bioreactor by reducing the gravitational forces[13]. Based on these data, we evaluated LCN2 in healthy volunteers, subjected to HDBR, an analogue model used to mimic microgravity-induced bone and muscle loss. This trial was originally designed to investigate the association between high NaCl intake, concomitant with a low-grade metabolic acidosis, and exacerbated bone resorption and protein wasting[14]. We took advantage of unutilized study samples and found that the serum LCN2 levels were higher after HDBR if compared to basal levels (time 0) (Fig. 1), revealing direct correlation between LCN2 levels and time of HDBR. Changes were not associated to sodium intake as suggested by the lack of statistical significance between the low (Fig. 1, black symbols) and the high (Fig. 1, open symbols) sodium intake groups at each time point. Induction of LCN2 was progressive and achieved statistical significance after 12 days of HDBR (Fig. 1). In agreement with our previous *in vitro* findings, that demonstrated an increase of LCN2 in primary osteoblasts picking after 5 days of unloading[13], we can conclude that LCN2 induction is not an early event as it requires days of stimulation by decreased mechanical forces.

### LCN2 expression in the bones of animal models subjected to unloading condition

The evidence in humans, together with the *in vitro* results previously obtained in isolated murine osteoblasts[13], prompted us to further characterize the relationship between *Lcn2* expression and the response of bone to reduced mechanical forces in animal models. We first employed the tail suspension of mice as a model of hindlimb unloading[15] and found that the mRNA expression of *Lcn2* significantly increased in the bones of the suspended hindlimbs with respect to those of the hindlimbs of mice maintained under normal conditions, employed as controls (Fig. 2A).

Noteworthy, this increase was antagonized by physical exercise through the forced swimming test (Fig. 2A).

To identify the cell lineage producing more LCN2 in tail suspended mice, we performed a FACS analysis of bone marrow cells flushed out from femurs. We found that the $CD45^-$ subpopulation, known to represent the bone marrow stromal cells and to include the osteoblast lineage, was the only one responding to the unloading conditions by increasing its LCN2 expression. This increase was again antagonized by the physical exercise (Fig. 2B).

Next we asked whether the biomechanical properties of the bones of these mice, known to be impaired by unloading (Fig. 2C,D), correlated with the *Lcn2* modulation. Indeed, the regression test showed a direct correlation between *Lcn2* transcriptional expression and the total indentation distance (Fig. 2E), a parameter that increases when the bone quality is compromised.

We have previously reported that dystrophic homozygous MDX mice[17] are characterized by an osteopenic phenotype[18]. In these mice we analyzed the *Lcn2* mRNA expression in bone and, consistent with the results of hindlimb suspension, we observed that it was significantly increased with respect to the WT littermates (Fig. 2F). This increase was prevented subjecting the MDX mice to physical exercise by treadmill running (Fig. 2F).

We next created an additional model of mechanical unloading injecting Botox in both quadriceps and calf muscles of the right hindlimbs of 5 week-old mice. This procedure induced a transient paralysis causing a dramatic alteration of muscle organization, as demonstrated by hematoxylin/eosin staining of muscle sections (Fig. 3A). As expected[16], this mechanical impairment induced a reduction of bone volume/total tissue volume (Fig. 3B) and trabecular

number (Figure 3C), no modulation of trabecular thickness (Fig. 3D) and an increase of trabecular separation (Fig. 3E). Histomorphometric analysis revealed an increase of osteoclast surface (Fig. 3F), together with a decrease of osteoblast surface (Fig. 3G) over bone surface and a trend of increase of bone marrow adiposity (Fig. 3H,I). Again, under this loading constrain we observed a significant increase of LCN2 both at protein (Fig. 4A) and transcriptional (Fig. 4B) level. Consistently, serum level of LCN2 was time-dependently increased in Botox-treated mice compared to control mice (Fig. 4C). Biomechanical tests confirmed impaired mechanical properties induced by unloading (Fig. 4D,E), while regression tests evidenced that *Lcn2* mRNA level had a direct correlation with the reduction of mechanical strength (Fig. 4F) and an inverse correlation with the bone volume/total tissue volume (Fig. 4G).

To address whether high *Lcn2* levels were involved in bone mass loss also independently of mechanical unloading, we evaluated *Lcn2* expression in ovariectomized (OVX) mice and observed that, in this circumstance, *Lcn2* expression was significantly reduced both at transcriptional and protein level compared to sham operated mice (Supplementary Fig. 1A,B). This result suggests that LCN2 overexpression represents a specific response of bone to mechanical release.

**Role of LCN2 in osteoblast activity**

To dissect the role of LCN2 in osteoblast metabolism, mouse primary osteoblasts were transfected with *Lcn2*-expression-vector (OBs-LCN2) or with control empty vector (OBs-empty). Successful overexpression of LCN2 was confirmed at mRNA (Fig. 5A) and protein (Fig. 5B) levels by real time RT-PCR and ELISA assays, respectively. Interestingly, OBs-LCN2 exhibited a less differentiated phenotype, as indicated by a lower transcriptional expression of *Alp* (Fig. 5C), *Runx2* (Fig. 5D) and *Osterix* (Fig. 5E) genes, compared to OBs-empty. Consistently, histochemical evaluation of ALP evidenced a lower activity in OBs-LCN2 *versus* OBs-empty (Fig. 5F). Primary

osteoblasts transfected with *Runx2* expression vector (Supplementary Fig. 2A) showed no change of *Lcn2* transcriptional level (Supplementary Fig. 2B), implying that *Lcn2* is likely to represent a primary osteoblast gene not subjected to *Runx2* regulation. Finally, in OBs-LCN2 we observed an increase of phosphorylated ERK, suggesting the involvement of the MAPK pathway in the LCN2 signaling (Fig.5G). Accordingly, osteoblasts expressed both LCN2 receptors, 24p3R and megalin (Fig 5H,I) which, however, were not modulated during osteoblast differentiation as demonstrated by the lack of correlation with the osteoblast differentiating genes *Alp* and *Runx 2*, and with *Lcn2* itself (Supplementary Fig. 2C). These results support a dominant role of LCN2 in causing the poor osteoblast differentiation observed in our previous study performed under simulated microgravity[24] and underscore the involvement of a receptor-mediated mechanism associated to the ERK pathway.

**Role of LCN2 on osteoclast activity**

Since osteoblasts are the main players in the regulation of osteoclast formation and function, we asked whether LCN2 overexpression could interfere with the paracrine production of osteoclast regulating cytokines. In line with this hypothesis, we observed that OBs-LCN2 produced a significantly higher amount of the osteoclastogenic cytokines *Receptor Activator of Nuclear Factor Kappa B Ligand* (*RankL)* (Figure 6A) and *InterLeukin 6* (*IL6*) (Fig. 6B), and a lower expression of the RANKL decoy receptor *Osteoprotegerin* (*Opg*) (Fig. 6C), thus leading to a significant increase of the *RankL*/*Opg* ratio (Fig. 6D).

These results prompted us to investigate whether LCN2 could indirectly affect osteoclastogenesis by treating mouse bone marrow mononuclear cells with conditioned media collected from OBs-LCN2 or OBs-empty. This experiment evidenced a significant increase of osteoclast number in the presence of conditioned medium from OBs-LCN2 (Fig. 6E). Similar results were observed in purified bone marrow mononuclear cells co-cultured with OBs-LCN2 relative to OBs-empty (Fig.

6F). This osteoclastogenic effect was not due to the LCN2 itself because the treatment of pre-osteoclast cultures with rmLCN2 failed to increase osteoclastogenesis over control (Fig. 6G).

In order to address whether LCN2 overexpression could induce similar changes in a cell type not correlated with bone, we transfected the human epithelial cell line HEK293 with empty- or LCN2-carrying vectors (Fig. 7A). Under this condition, increased LCN2 also induced *RankL* mRNA expression (Fig. 7B), with albeit no effects on *Opg* expression (Fig. 7C). Nevertheless, the *RankL* change led to a significant increase of the *RankL/Opg* ratio (Fig. 7D). In contrast, we did not observe any regulation of *IL-6* mRNA level (Fig.7E).

Consistent with the induction of *RankL,* enhanced osteoclast formation was demonstrated in experiments in which purified bone marrow mononuclear cells were cultured in the presence of conditioned medium from HEK293 cells transfected with control or LCN2 vector (Figure 7F). This effect was blunted by treatment with OPG (Figure 7G), confirming that it was due to the increased RANKL concentration in the conditioned medium of LCN2 overexpressing cells.

## DISCUSSION

LCN2 is a very versatile molecule that plays different roles in several cell types and conditions. It has recently been the subject of a great interest as an early biomarker not only in renal injury but also in several other conditions, including cancer, anemia, pregnancy and cardiovascular diseases[25-28]. The multifaceted roles of LCN2 are well evident in tumor cells, where the proposed functions range from inhibiting apoptosis[29], invasion and angiogenesis[30], to increasing proliferation and metastasis[31,32]. Ectopic expression of LCN2 also promotes BCR-ABL-induced chronic myelogenous leukemia in murine models[33]. Moreover, it forms a complex with the proteolytic enzyme matrix metalloprotease-9 (MMP-9), thus preventing its degradation[34].

Despite these many different functions, the role of LCN2 in bone metabolism is still unclear and only recently some researches are starting to elucidate it. Costa and colleagues showed an increased expression of SDF-1 in transgenic mice overexpressing LCN2 specifically in osteoblasts under the control of a type I collagen promoter, that correlated with an increased number of CD34+/CXCR4+ (SDF-1 receptor) cells[35]. These mice also exhibited growth plate defect, reduced bone mass, delayed osteoblast differentiation and enhanced osteoclast activity, thus supporting our observations[36]. In fact, in our hands, LCN2 appears to have a crucial role especially in conditions associated to a decrease of mechanical forces. Our previous work[13] demonstrated that osteoblasts progressively up-regulate LCN2 expression in a manner proportional to the reduction of gravitational force intensity. Interestingly, in the present study, we demonstrated a direct correlation between LCN2 serum levels and the mechanical unloading mimicked in human subjects by HDBR condition. These results were also confirmed *in vivo* in the long bones of various animal models of mechanical unloading, strongly indicating a causative role of LCN2 in inducing bone loss. Noteworthy, Miravète et al.[37] suggested a role of LCN2 in urinary fluid shear stress-induced alterations observed in early phases of most kidney diseases, confirming the mechanoresponding

properties of this gene also in another context. Interestingly, our data indicate that increased *Lcn2* expression is specifically associated to unloading-induced bone loss. In fact, contrariwise, in ovariectomized (OVX) mice, which typically reproduce a condition of bone loss independent of mechanical forces, we found a significant reduction of LCN2 compared to sham operated mice. These data suggest that LCN2 could play an alternative role in postmenopausal osteoporosis, underscoring the need of further work to deeply understand its complex involvement in the context of bone metabolism.

Mechanistically, in vivo CD45- cells, known to belong to the stromal cellular component of the bone marrow that also includes the osteoblast lineage, were the major sources of LCN2 in unloading conditions. Furthermore, increased LCN2 levels matched with an inhibition of osteoblast differentiation, as demonstrated by our *in vitro* study, where the overexpression of LCN2 alone in osteoblasts sufficed to inhibit their differentiation. In fact, crucial osteoblast genes such as *Runx2*, *Osterix* and *Alp*, which were previously noted to be down-regulated under reduced mechanical forces *in vitro*[13], were blunted in osteoblasts overexpressing LCN2. Our results also suggest that LCN2 works upstream of the typical osteoblast master protein, Runx2, representing a novel primary osteoblast differentiation regulatory pathway.

Interestingly, LCN2 also appears to contribute to the osteoblast-osteoclast coupling. In fact, overexpression of LCN2 in osteoblasts increased their ability to stimulate osteoclastogenesis through the induction of the pro-osteoclastogenic factors, RANKL and IL-6, and the inhibition of the anti-osteoclastogenic factor, OPG. The induction of RANKL by LCN2 was observed also in a bone-unrelated cell line (HEK293). Consistently, HEK293 cell conditioned medium had pro-osteoclastogenic properties fully blocked by treatment with the RANKL-decoy receptor, OPG. In contrast, LCN2 did not exhibit pro-osteoclastogenic properties itself, suggesting a dominant role

only in osteoblasts, which reliably expressed both LCN2 receptors, megalin and 24P3R, and responded to LCN2 overexpression through the ERK pathway.

In conclusion, we believe that LCN2 is an important osteoblast mechanoresponding gene with a role in bone metabolism, that could be involved in the onset of osteoporosis induced by mechanical failures due for instance to disuse, bed rest, muscle impairment or aging, decreasing osteoblast differentiation and increasing osteoblast-induced osteoclastogenesis. These results open new perspective in the understanding of the molecular mechanisms governing bone metabolism under stimulation by mechanical forces in physiologic and pathologic conditions, and establish a track for diagnostic and therapeutic developments also in humans.

**ACKNOWLEDGEMENTS**

We are indebted with Dr. Rita Di Massimo for her excellent contribution in writing this manuscript.

**AUTHORS' ROLE**

Study design: NR, MC, AT. Study conduct: NR, MC, AC, SGP, PL, PFM, MH, AT. Data collection: NR, MC, AC, AT. Data analysis: NR, MC, AC, AT. Data interpretation: NR, MC, AT. Drafting manuscript: NR, AT. Revising manuscript content: NR, MC, AT. Approving final version of manuscript: NR, MC, AC, SGP, PL, PFM, MH, AT. NR takes responsibility for the integrity of the data analysis.

## REFERENCES


1. Kjeldsen L, Johnsen AH, Sengelov H, Borregaard N. Isolation and primary structure of NGAL, a novel protein associated with human neutrophil gelatinase. J Biol Chem. 1993; 268:10425-432.
2. Kjeldsen L, Bainton DF, Sengelov H, Borregaard N. Identification of neutrophil gelatinase-associated lipocalin as a novel matrix protein of specific granules in human neutrophils. Blood 1994;83:799–807.
3. Goetz DH, Holmes MA, Borregaard N, Bluhm ME, Raymond KN, Strong RK. The neutrophil lipocalin NGAL is a bacteriostatic agent that interferes with siderophore-mediated iron acquisition. Mol Cell. 2002;10:1033–43.
4. Flo TH, Smith KD, Sato S, Rodriguez DJ, Holmes MA, Strong RK et al. Lipocalin 2 mediates an innate immune response to bacterial infection by sequestrating iron. Nature 2004; 32:917–21.
5. Berger T, Togawa A, Duncan GS, Elia AJ, You-Ten A, Wakeham A et al. Lipocalin 2-deficient mice exhibit increased sensitivity to Escherichia coli infection but not to ischemia-reperfusion injury. Proc Natl Acad Sci USA 2006;103:1834-39.
6. Wang Y, Lam KS, Kraegen EW, Sweeney G, Zhang J, Tso AW et al. Lipocalin-2 is an inflammatory marker closely associated with obesity, insulin resistance, and hyperglycemia in humans. Clin Chem. 2007;53:34–41.
7. Yan QW, Yang Q, Mody N, Graham TE, Hsu CH, Xu Z et al. The adipokine lipocalin 2 is regulated by obesity and promotes insulin resistance. Diabetes 2007;56:2533–40.
8. Choi KM, Lee JS, Kim EJ, Baik SH, Seo HS, Choi DS et al. Implication of lipocalin-2 and visfatin levels in patients with coronary heart disease. Eur J Endocrinol.2008;158:203–7-

9. Schmidt-Ott KM, Mori K, Kalandadze A, Li JY, Paragas N, Nicholas T et al. Neutrophil gelatinase associated lipocalin-mediated iron traffic in kidney epithelia. Curr Opin Nephrol Hypertens. 2006;15:442–9.
10. Devireddy LR, Gazin C, Zhu X, Green MR. A cell-surface receptor for lipocalin 24p3 selectively mediates apoptosis and iron uptake. Cell 2005;123:1293-1305.
11. Hvidberg V, Jacobsen C, Strong RK, Cowland JB, Moestrup SK, Borregaard N**.** The endocytic receptor megalin binds the iron transporting neutrophil-gelatinase-associated lipocalin with high affinity and mediates its cellular uptake. FEBS Lett. 2005;579:773-7.
12. Mori K, Lee HT, Rapoport D, Drexler IR, Foster K, Yang J et al. Endocytic delivery of lipocalin-siderophore-iron complex rescues the kidney from ischemia-reperfusion injury. J Clin Invest. 2005;115:610–21.
13. Capulli M, Rufo A, Teti A, Rucci N. Global transcriptome analysis in mouse calvarial osteoblasts highlights sets of genes regulated by modeled microgravity and identifies a "mechanoresponsive osteoblast gene signature". J Cell Biochem. 2009;107:240-52.
14. Frings-Meuthen P, Buehlmeier J, Baecker N, Stehle P, Fimmers R, May F et al. High sodium chloride intake exacerbates immobilization-induced bone resorption and protein losses. J Appl Physiol. 2011;111:537-42.
15. Sakata T, Sakai A, Tsurukami H, Okimoto N, Okazaki Y, Ikeda S. et al. Trabecular bone turnover and bone marrow cell development in tail-suspended mice. J Bone Miner Res. 1999;14:1596-1604.
16. Warner SE, Sanforda DA, Beckera BL, Bainb SD, Srinivasana S, Grossa TS. Botox induced muscle paralysis rapidly degrades bone. Bone 2006;38:257-64.
17. Bulfield G, Siller WG, Wight PA, Moore KJ. X chromosome-linked muscular dystrophy (mdx) in the mouse. Proc Natl Acad Sci U S A 1984;81:1189–92.

18. Rufo A, Del Fattore A, Capulli M, Carvello F, De Pasquale L, Ferrari S et al. Mechanisms inducing low bone density in Duchenne muscular dystrophy in mice and humans. J Bone Miner Res. 2011;26:1891-1903.
19. Goes ATR, Souza LC, Filho CB, Del Fabbro L, De Gomes MG, Boeira SP, Jesse CR. Neuroprotective effects of swimming training in a mouse model of Parkinson's disease induced by 6-hydroxydopamine. Neuroscience 2014;256:61-71.
20. Lorensen WE, Cline HE. Marching cubes: a high resolution 3d surface construction algorithm. Computer Graphics 1987;21:163-9.
21. Bouxsein ML, Boyd SK, Christiansen BA, Guldberg, RE, Jepsen KJ, Müller R. Guidelines for assessment of bone microstructure in rodents using micro-computed tomography. J Bone Miner Res 2010;25:1468-86.
22. Rucci N, Rufo A, Alamanou M, Capulli M, Del Fattore A, Ahrman E, Capece D, Iansante V, Zazzeroni F, Alesse E, Heinegård D, Teti A. The glycosaminoglycan-binding domain of PRELP acts as a cell type-specific NF-kappaB inhibitor that impairs osteoclastogenesis. J Cell Biol 2009;187:669-83.
23. Dempster DW, Compston JE, Drezner MK, Glorieux FH, Kanis J., Malluche H, Meunier PJ, Ott SM, Recker RR, Parfitt AM. Standardized nomenclature, symbols, and units for bone histomorphometry: A 2012 update of the report of the ASBMR Histomorphometry Nomenclature Committee. J Bone Miner Res 2013;28:2–17.
24. Rucci N, Rufo A, Alamanou M, Teti A. Modeled microgravity stimulates osteoclastogenesis and bone resorption by increasing osteoblast RANKL/OPG ratio. J Cell Biochem. 2007;100:464-73.
25. Makris K, Rizos D, Kafkas N, Haliassos A. Neurophil gelatinase-associated lipocalin as a new biomarker in laboratory medicine. Clin Chem Lab Med. 2012;50:1519-32.

26. Bolignano D, Donato V, Lacquaniti A, Fazio MR, Bono C, Coppolino G et al. Neutrophil gelatinase-associated lipocalin (NGAL) in human neoplasias: a new protein enters the scene. Cancer Lett 2010;288:10–16.
27. Huang HL, Chu ST, Chen YH. Ovarian steroids regulate 24p3 expression in mouse uterus during the natural estrous cycle and the preimplantation period. J Endocrinol. 1999;162:11–19.
28. D'Anna R, Baviera G, Corrado F, Giordano D, Recupero S, Di BA. First trimester serum neutrophil gelatinase-associated lipocalin in gestational diabetes. Diabet Med. 2009; 26:1293–95.
29. Iannetti A, Pacifico F, Acquaviva R, Lavorgna A, Crescenzi E, Vascotto C. The neutrophil gelatinase-associated lipocalin (NGAL), a NF-kappaB-regulated gene, is a survival factor for thyroid neoplastic cells. *Proc Natl Acad Sci USA* 2008;105:14058-63.
30. Moniaux N, Chakraborty S, Yalniz M, Gonzalez J, Shostrom VK, Standop J et al. Early diagnosis of pancreatic cancer: neutrophil gelatinase associated lipocalin as a marker of pancreatic intraepithelial neoplasia. Br J Cancer 2008; 98:1540–47.
31. Sun Y, Yokoi K, Li H, Gao J, Hu L, Liu B et al. NGAL expression is elevated in both colorectal adenoma-carcinoma sequence and cancer progression and enhances tumorigenesis in xenograft mouse models. Clin Cancer Res. 2011;17:4331–40.
32. Bauer M, Eickhoff JC, Gould MN, Mundhenke C, Maass N, Friedl A. Neutrophil gelatinase-associated lipocalin (NGAL) is a predictor of poor prognosis in human primary breast cancer. Breast Cancer Res Treat. 2008;108:389–397.
33. Leng X, Lin H, Ding T, Wang Y, Wu Y, Klumpp S et al. Lipocalin 2 is required for BCR-ABL-induced tumorigenesis. Oncogene 2008;27:6110–19.
34. Yan L, Borregaard N, Kjeldsen L, Moses MA. The high molecular weight urinary matrix metalloproteinase (MMP) activity is a complex of gelatinase B/MMP-9 and neutrophil

gelatinase-associated lipocalin (NGAL). Modulation of MMP-9 activity by NGAL. J Biol Chem. 2001;276:37258–65.

35. Costa D, Biticchi R, Negrini S, Tasso R, Cancedda R, Descalzi F et al. Lipocalin-2 controls the expression of SDF-1 and the number of responsive cells in bone. Cytokine 2010;51:47-52.

36. Costa D, Lazzarini E, Canciani B, Giuliani A, Spanò R, Marozzi K et al. Altered bone development and turnover in transgenic mice over-expressing lipocalin-2 in bone. J Cell Physiol. 2013;228:2210-21.

37. Miravète M, Dissard R, Klein J, Gonzalez J, Caubet C, Pecher C, Pipy B, Bascands JL, Mercier-Bonin M, Schanstra JP, Buffin-Meyer B. Am J Physiol Renal Physiol. 2012; 302:F1409-17.

**Table 1**: Primer pairs employed for comparative real time and semiquantitative RT-PCR.

| Gene | Primers | |
|---|---|---|
| | **Forward** | **Reverse** |
| *GAPDH* | 5'-TGGCAAAGTGGAGATTGTTGC -3' | 5'-AAGATGGTGATGGGCTTCCCG -3' |
| *Lcn 2* | 5'-CCAGTTCGCCATGGTATTTT-3' | 5'-CACACTCACCACCCATTCAG-3' |
| *Alp* | 5'-CCAGCAGGTTTCTCTCTTGG-3' | 5'-CTGGGAGTCTCATCCTGAGC-3' |
| *Runx2* | 5'-AACCCACGGCCCTCCCTGAACTCT-3' | 5'-ACTGGCGGGGTGTAGGTAAAGGTG-3' |
| *Osterix* | 5'-TGCTTCCCAATCCTATTTGC-3' | 5'-AGAATCCCTTTCCCTCTCCA-3' |
| *IL-6* | 5'-GAGGATACCACTCCCAACAGACC-3' | 5'-AAGTGCATCATCGTTGTTCATACA-3' |
| *RankL* | 5'-CCAAGATCTCTAACATGACG-3' | 5'-CACCATCAGCTGAAGATAGT-3' |
| *Opg* | 5'-AAAGCACCCTGTAGAAAACA-3' | 5'-CCGTTTTATCCTCTCTACACTC -3' |

PCR conditions were 94°C 30 sec, 60°C 30 sec, 72°C 30 sec, replicated for 40 cycles for real time RT-PCR and 27 cycles for semiquantitative RT-PCR.

## FIGURE LEGENDS

**Figure 1: LCN2 expression in sera of patients subjected to prolonged head-down tilt bed rest (HDBR). (A)** ELISA assay for human LCN2 performed in sera of 8 healthy volunteers subjected to HDBR (15 days). Sera were collected just before the HDBR (day 0) and during the HDBR (days 1, 3, 6, 8, 11, 15). Open squares: 500 mmoles NaCl/day, black squares: 50 mmoles NaCl/day. *P=0.003 and **P=0.001 *versus* day 0; differences between 500 mmoles NaCl/day and 50 mmoles NaCl/day are statistically not significant, with P>0.21 (paired *t*-test).

**Figure 2: Effect of *in vivo* mechanical unloading on LCN2 expression.** Eight week-old mice were maintained in Normal Loading Conditions (NLC) or were subjected to HindLimb Suspension (HLS) for 21 days. A group of them was subjected to physical Exercise (HLS+E) (forced swimming test) during the experiment of unloading, as described in Materials and Methods. **(A)** Transcriptional evaluation of *Lcn2* expression in the hindlimb bones by comparative real time RT-PCR. **(B)** Evaluation by FACS analysis of the percent of $CD45^-/LCN2^+$ cells in the bone marrow. **(C)** Dissipated Energy (DE, μJ) and **(D)** Total Indentation Distance (TID, μm) in distal femurs. **(E)** Linear regression test showing a direct correlation between *Lcn2* mRNA and distal femoral TID. Data are the mean ± SD. *P< 0.038 and **P = 0.016 *versus* NLC (Non-parametric Mann-Whitney Runk Sum Test). **(F)** Transcriptional expression of *Lcn2* by comparative real time RT-PCR in eight week-old wild type (WT) and MDX (X chromosome-linked muscular dystrophy) mice, the latter maintained under sedentary conditions or subjected to physical Exercise (MDX+E) (treadmill running). $^{***}$P= 0.001 *versus* WT and $^{\#}$P=0.002 *versus* MDX (Non-parametric Mann-Whitney Runk Sum Test).

**Figure 3: Effect of transient paralysis on bone phenotype.** Eight week-old mice were injected with saline solution (vehicle) or with Botulin toxin A (Botox, 20 μl of 2.0 unit/100gr), into the right

quadriceps and the posterior compartment of the right calf (targeting gastrocnemius, plantaris, and soleus) 4 mm proximal to the patellar tendon of the left or the right hindlimbs, respectively. **(A)** Hematoxylin/eosin staining of muscle sections. **(B-E)** μCT analysis of proximal tibia spongiosa to quantify trabecular **(B)** bone volume/total tissue volume (BV/TV %), **(C)** number (TbN), **(D)** thickness (TbTh) and **(E)** separation (TbSp). **(F,G)** Histomorphometric analysis of proximal tibia to quantify **(F)** osteoclast surface/bone surface (OcS/BS) and **(G)** osteoblast surface/bone surface (ObS/BS). **(H)** Representative picture of femur sections stained with hematoxylin/eosin (B=bone, BM=bone marrow) and **(I)** quantification of the adipocyte number. *P<0.03, **P= 0.012 *versus* vehicle (unpaired *t*-test). In **(D)** and **(I)** data are statistically not significant, with P>0.1 and P=0.17 *versus* vehicle, respectively.

**Figure 4: Effect of transient paralysis on LCN2 transcriptional and protein expression.** Right quadriceps of 8 week-old mice injected with saline solution (vehicle) or with Botulin toxin A (Botox, 20 μl of 2.0 unit/100gr). **(A)** Immunocytochemistry for LCN2 detection in tibia sections (B=bone, BM=bone marrow). **(B)** Transcriptional expression of *Lcn2* by comparative real time RT-PCR. **(C)** Linear regression test showing a direct correlation between serum LCN2 levels and the duration of unloading. (**D**) Distal femur Dissipated Energy (DE, μJ) and (**E**) Total Indentation Distance (TID, μm). **(F,G)** Linear regression test showing **(F)** a direct correlation between *Lcn2* mRNA and the Total Indentation Distance, and **(G)** an inverse correlation between *Lcn2* mRNA and trabecular bone volume/total tissue volume (BV/TV).**P<0.04 *versus* vehicle (Non-parametric Mann-Whitney Runk Sum Test).

**Figure 5: Effect of LCN2 overexpression on osteoblast differentiation. (A-F)** AMAXA nucleofection of primary osteoblasts with LCN2 (OBs-LCN2) or with an empty vector as control (OBs-empty). **(A)** mRNA and **(B)** protein expressions of LCN2 performed by comparative real time

RT-PCR and ELISA assays, respectively. **(C-E)** Transcriptional expression of **(C)** *Alp*, **(D)** *Runx2* and **(E)** *Osterix* by comparative real time RT-PCR. **(F)** Quantification (graph) of ALP activity evaluated by histochemical assay (inset). **(G)** Western blot analysis of phosphorylated ERK (pERK) and total ERK. **(H)** mRNA and **(I)** protein expression of the LCN2 receptors, megalin and 24P3R, in primary osteoblasts evaluated by RT-PCR and immunofluorescence, respectively (Neg.Ctrl=negative control, immunofluorescence performed by omitting the primary antibody). Data are **(A-F)** the mean ± SD or **(G-I)** representative of three independent experiments. *P<0.05, **P=0.038 and ***P<0.003 *versus* OBs-empty (unpaired *t*-test).

**Figure 6: Effect of LCN2 overexpression on osteoclastogenesis. (A-D)** RNA from osteoblasts transfected with LCN2 (OBs-LCN2) or with the empty vector (OBs-empty) was extracted, retro-transcribed and subjected to comparative real time RT-PCR for **(A)** *RankL*, **(B)** *IL-6* and **(C)** *Opg* mRNAs evaluation. Data are normalized *versus* the housekeeping gene *Gapdh.* **(D)** *RankL/Opg* ratio. **(E)** Purified bone marrow mononuclear cells were treated with conditioned media (CM) from osteoblasts transfected with LCN2 (OBs-LCN2-CM) or with the empty vector (OBs-empty-CM) in the presence of M-CSF and suboptimal concentrations of RANKL for 7 days. **(F)** OBs-empty and OBs-LCN2 cells were co-cultured with purified mouse bone marrow mononuclear cells for 7 days. **(G)** Purified bone marrow mononuclear cells were treated with rmLcn2 (100ng/ml). At the end of the experiment, mature osteoclasts were detected by TRAcP histochemical staining. Results are the mean ± SD of three independent experiments. *P<0.02 and **P=0.0026 *versus* OBs-empty; #P=0.0028 *versus* OBs-empty-CM; in **(F)** P=0.06 *versus* OBs-empty (unpaired *t* test).

**Figure 7: LCN2 overexpression in HEK293 cells.** HEK293 cells were transfected with an empty vector (HEK-empty) or with a construct carrying LCN2 (HEK-LCN2). Cells were collected, the

RNA was extracted, reverse-transcribed and subjected to comparative real time RT-PCR, using primer pairs and conditions specific for **(A)** *Lcn2,* **(B)** *RankL* and **(C)** *Opg*. In **(D)** the *Rankl/Opg* ratio was calculated. Results are reported as fold increase and are normalized *versus* the housekeeping gene *GAPDH*. **(E)** Human peripheral blood mononuclear cells (hPBMCs) obtained by Ficoll separation were allowed to differentiate into osteoclasts in the presence of M-CSF, suboptimal concentrations of RANKL and conditioned media from HEK293 cells transfected with empty vector (HEK-empty-CM) or with LCN2 (HEK-LCN2-CM). **(F)** hPBMCs, were allowed to differentiate into osteoclasts as described in **(E)**, with or without osteoprotegerin (OPG). Data are the mean ± SD of three independent experiments. *P < 0.05 and **P < 0.005 *versus* HEK-empty; $^{\$}$P < 0.05 *versus* HEK-empty-CM and $^{\#}$P< 0.04 *versus* HEK-empty-CM and HEK-LCN2-CM (unpaired *t* test).

1

2

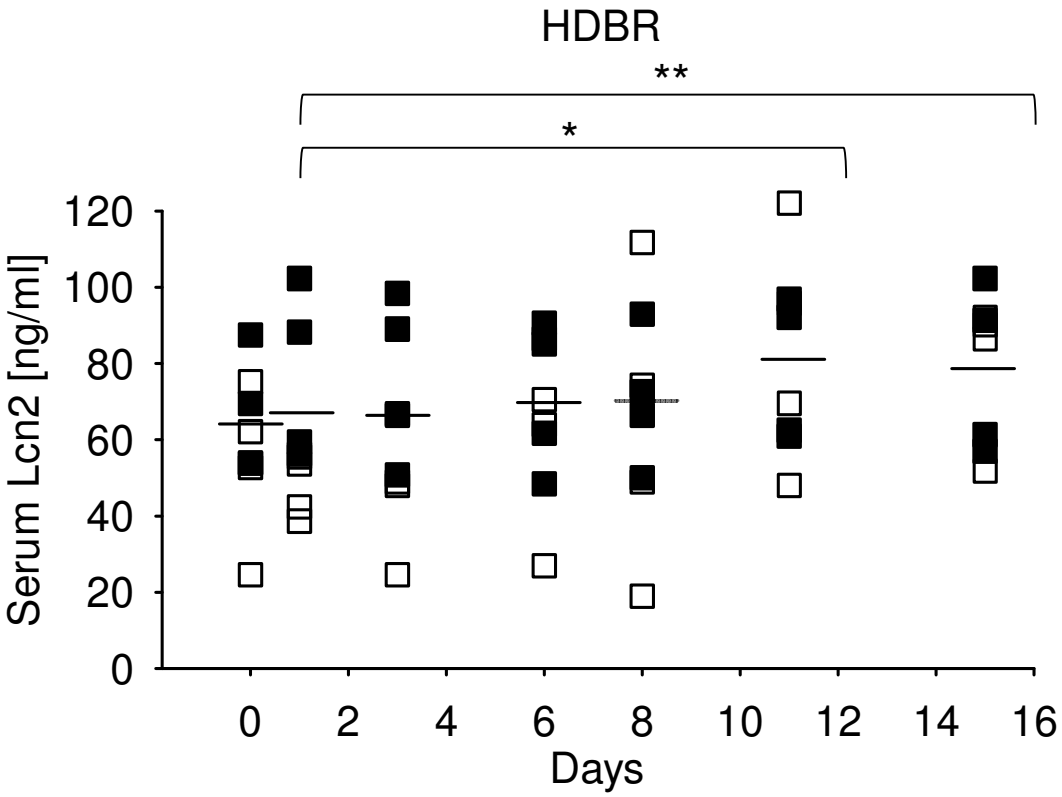




Figure 1

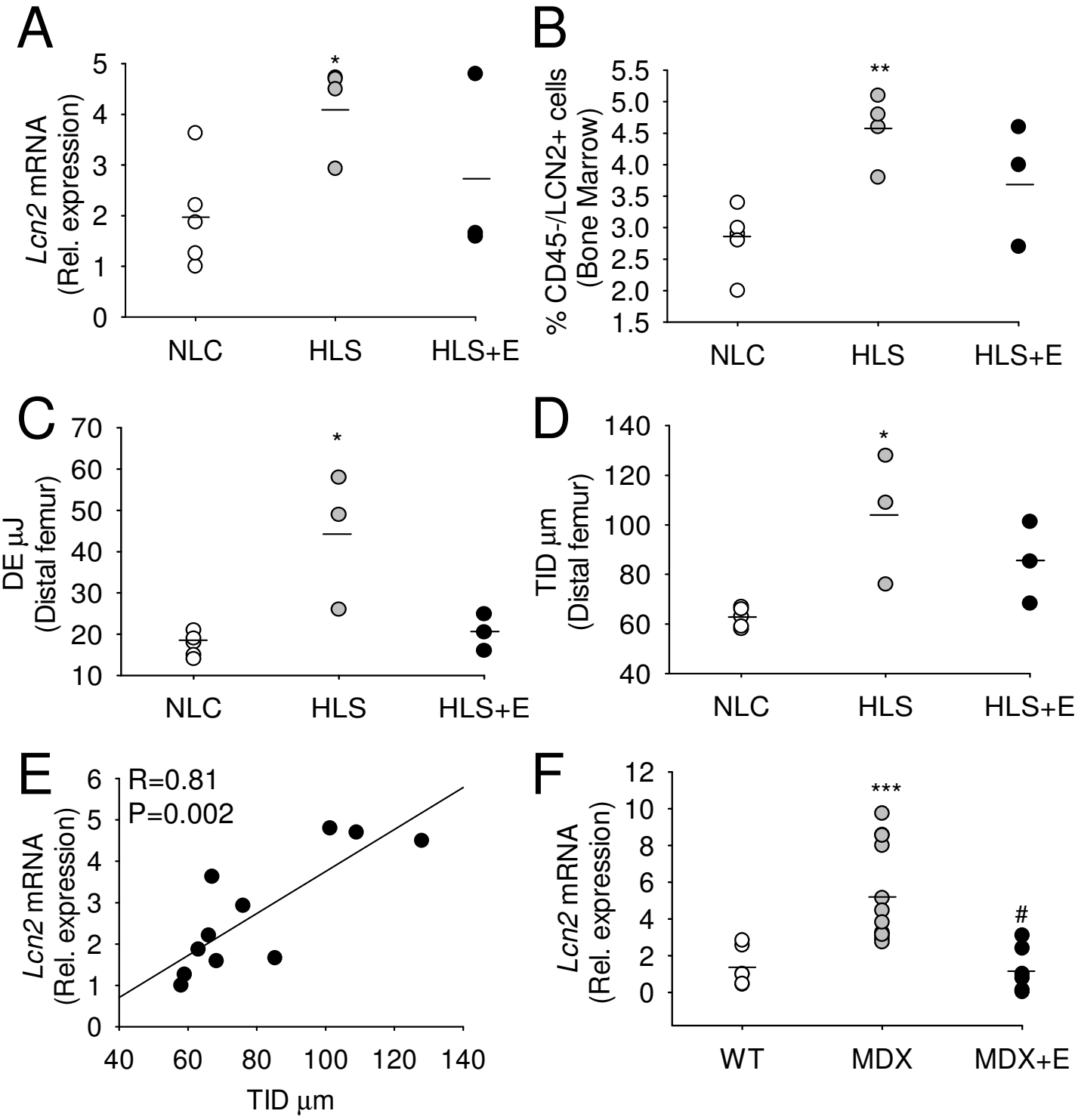
A
Lcn2 mRNA (Rel. expression)
0
1
2
3
4
5
*
NLC
HLS
HLS+E
B
% CD45-/LCN2+ cells (Bone Marrow)
1.5
2.0
2.5
3.0
3.5
4.0
4.5
5.0
5.5
**
NLC
HLS
HLS+E
C
DE µJ (Distal femur)
10
20
30
40
50
60
70
*
NLC
HLS
HLS+E
D
TID µm (Distal femur)
40
60
80
100
120
140
*
NLC
HLS
HLS+E
E
R=0.81
P=0.002
Lcn2 mRNA (Rel. expression)
0
1
2
3
4
5
6
40
60
80
100
120
140
TID µm
F
Lcn2 mRNA (Rel. expression)
0
2
4
6
8
10
12
***
#
WT
MDX
MDX+E



Figure 2

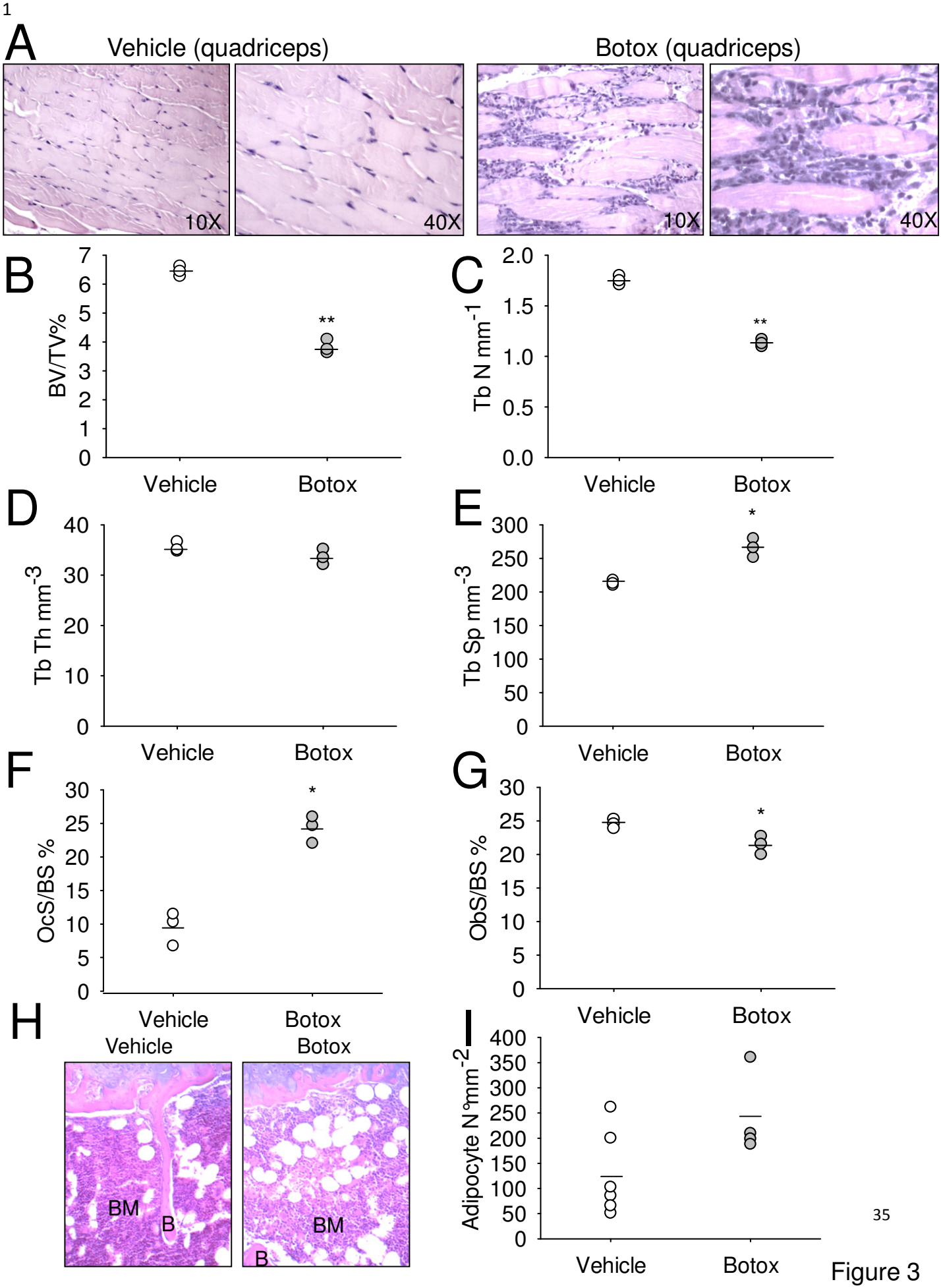
A
Vehicle (quadriceps)
Botox (quadriceps)
10X
40X
10X
40X
B
BV/TV%
**
Vehicle
Botox
C
Tb N mm-1
**
Vehicle
Botox
D
Tb Th mm-3
Vehicle
Botox
E
Tb Sp mm-3
*
Vehicle
Botox
F
OcS/BS %
*
Vehicle
Botox
G
ObS/BS %
*
Vehicle
Botox
H
Vehicle
Botox
BM
B
BM
B
I
Adipocyte N°mm-2
Vehicle
Botox



Figure 3

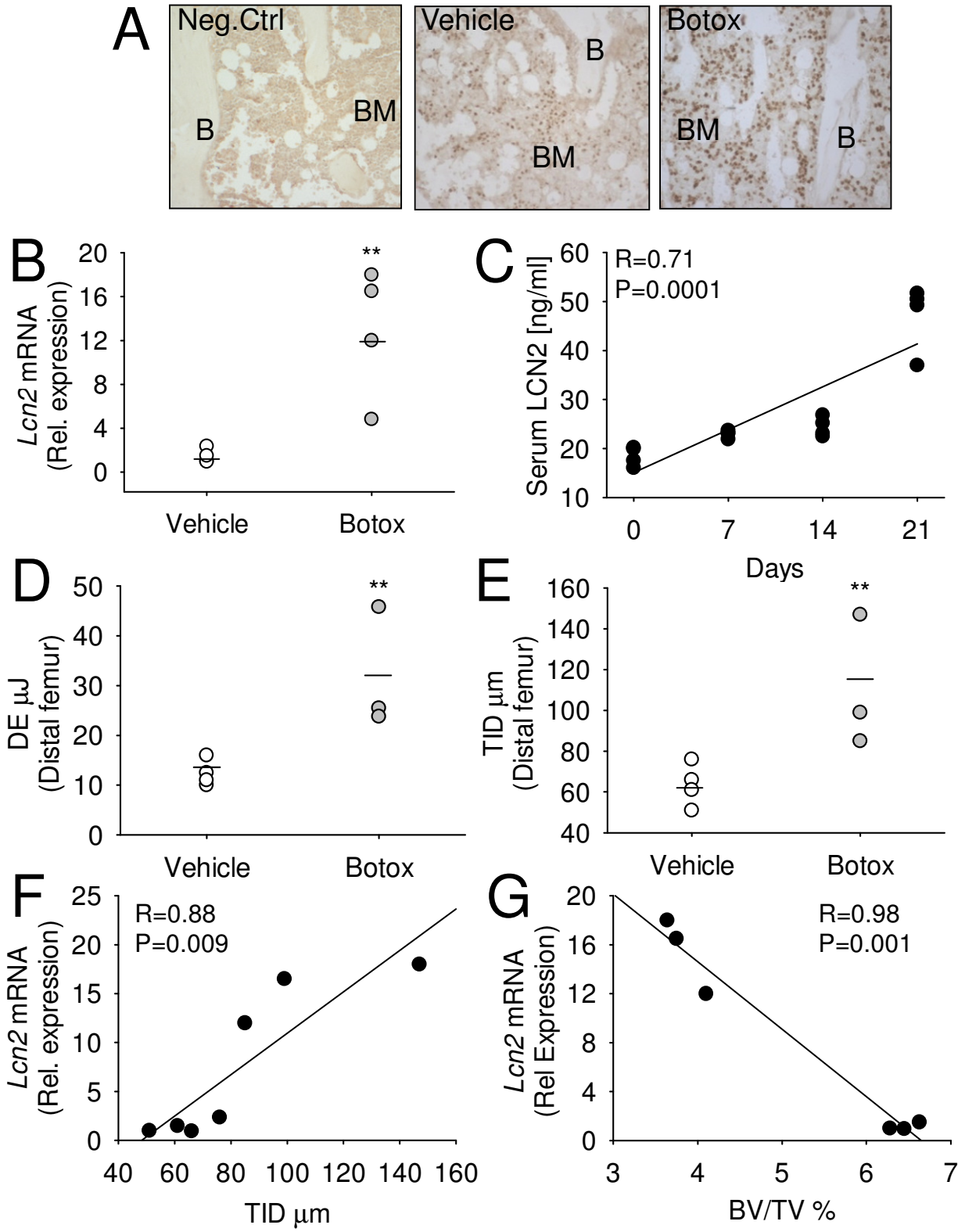
A
Neg.Ctrl
B
BM
Vehicle
B
BM
Botox
BM
B
B
Lcn2 mRNA (Rel. expression)
**
Vehicle
Botox
C
R=0.71
P=0.0001
Serum LCN2 [ng/ml]
Days
D
DE µJ (Distal femur)
**
Vehicle
Botox
E
TID µm (Distal femur)
**
Vehicle
Botox
F
R=0.88
P=0.009
Lcn2 mRNA (Rel. expression)
TID µm
G
R=0.98
P=0.001
Lcn2 mRNA (Rel Expression)
BV/TV %

Figure 4

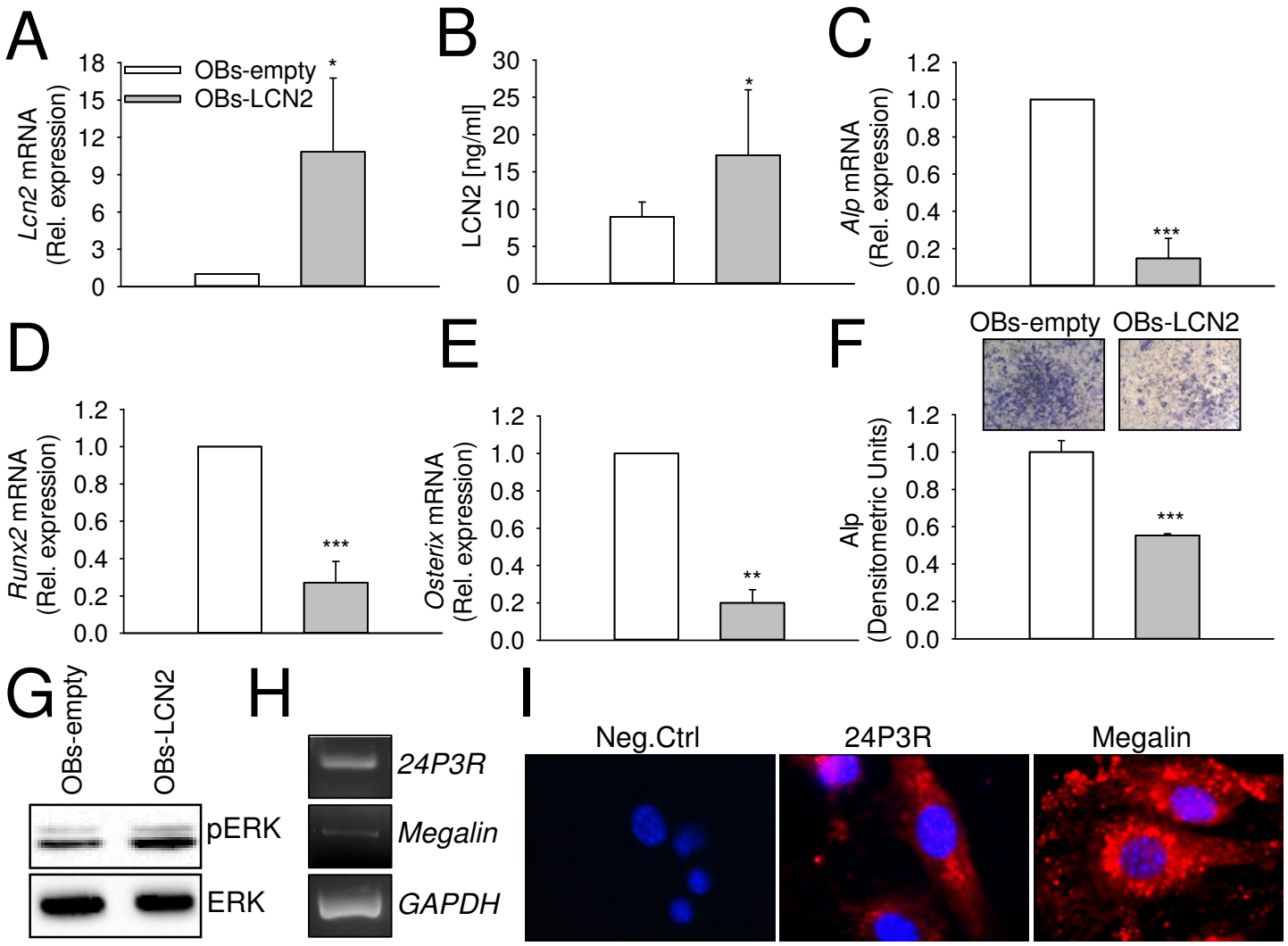
A
B
C
D
E
F
G
H
I
OBs-empty
OBs-LCN2
Lcn2 mRNA (Rel. expression)
LCN2 [ng/ml]
Alp mRNA (Rel. expression)
Runx2 mRNA (Rel. expression)
Osterix mRNA (Rel. expression)
Alp (Densitometric Units)
pERK
ERK
24P3R
Megalin
GAPDH
Neg.Ctrl
24P3R
Megalin

Figure 5

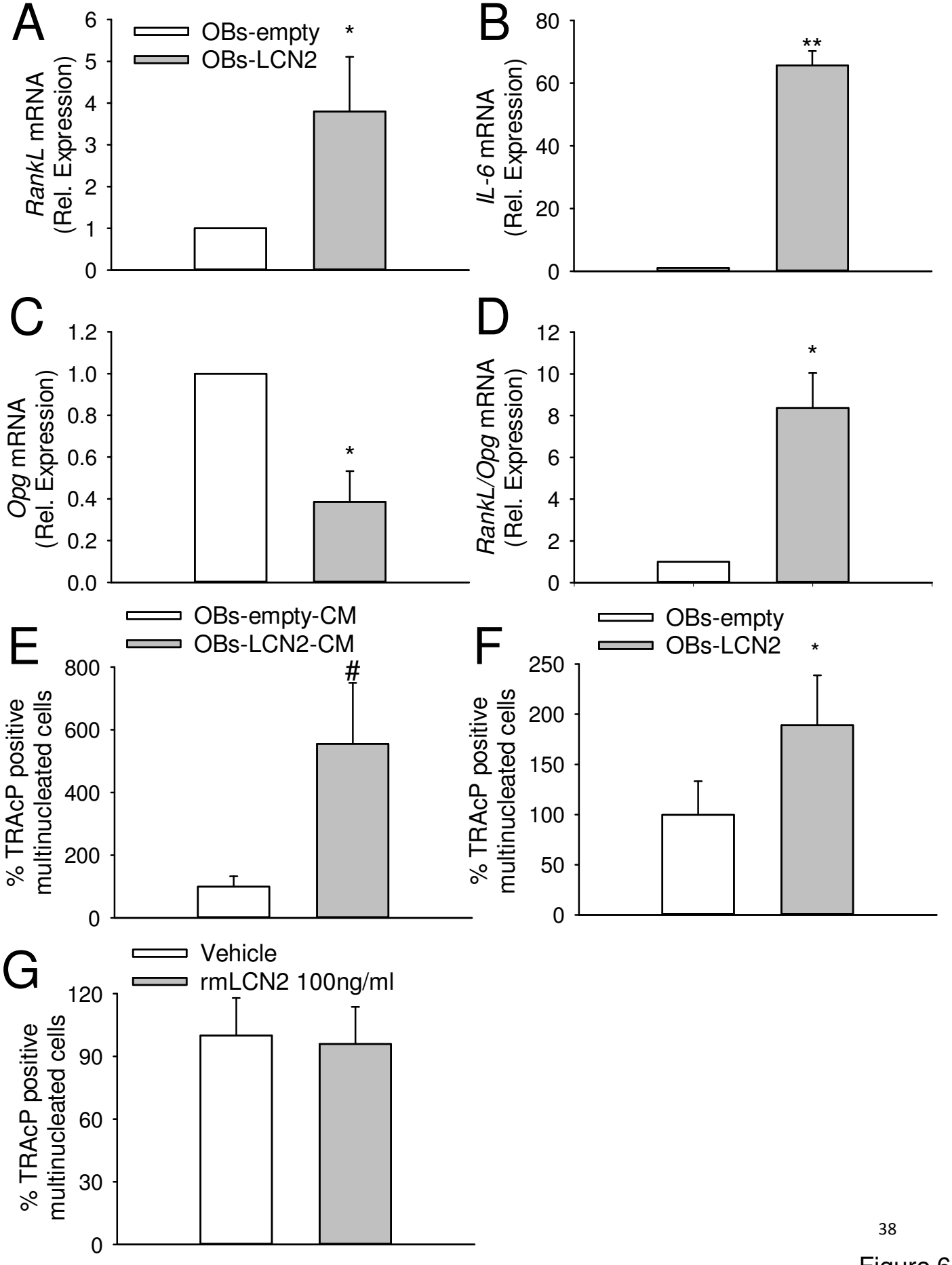
A
OBs-empty
OBs-LCN2
*
RankL mRNA (Rel. Expression)
0
1
2
3
4
5
6
B
**
IL-6 mRNA (Rel. Expression)
0
20
40
60
80
C
*
Opg mRNA (Rel. Expression)
0.0
0.2
0.4
0.6
0.8
1.0
1.2
D
*
RankL/Opg mRNA (Rel. Expression)
0
2
4
6
8
10
12
E
OBs-empty-CM
OBs-LCN2-CM
#
% TRAcP positive multinucleated cells
0
200
400
600
800
F
OBs-empty
OBs-LCN2
*
% TRAcP positive multinucleated cells
0
50
100
150
200
250
G
Vehicle
rmLCN2 100ng/ml
% TRAcP positive multinucleated cells
0
30
60
90
120



Figure 6

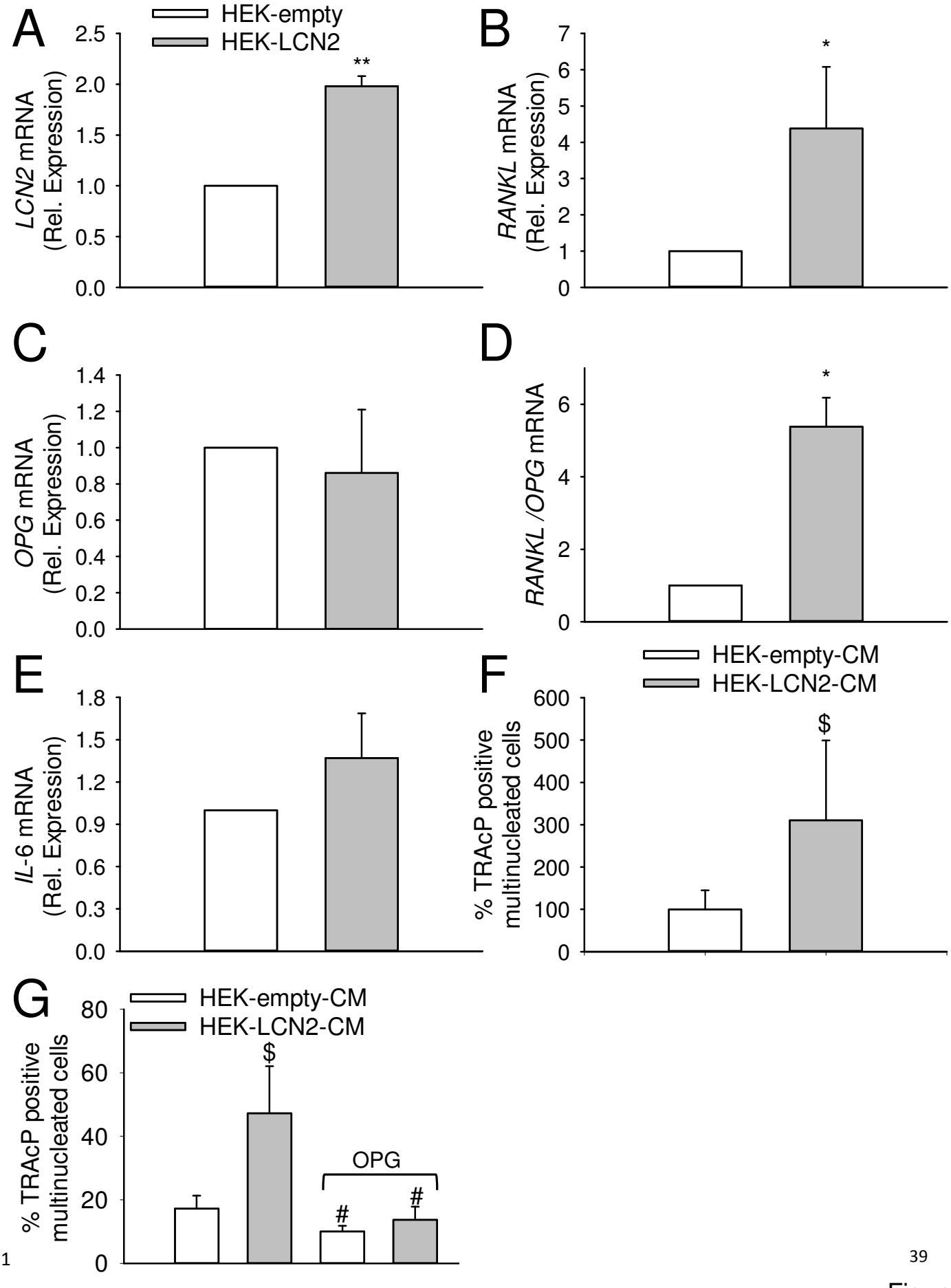
A
HEK-empty
HEK-LCN2
LCN2 mRNA (Rel. Expression)
2.5
2.0
1.5
1.0
0.5
0.0
**
B
RANKL mRNA (Rel. Expression)
7
6
5
4
3
2
1
0
*
C
OPG mRNA (Rel. Expression)
1.4
1.2
1.0
0.8
0.6
0.4
0.2
0.0
D
RANKL /OPG mRNA
6
4
2
0
*
E
IL-6 mRNA (Rel. Expression)
1.8
1.5
1.2
0.9
0.6
0.3
0.0
F
HEK-empty-CM
HEK-LCN2-CM
% TRAcP positive multinucleated cells
600
500
400
300
200
100
0
$
G
HEK-empty-CM
HEK-LCN2-CM
% TRAcP positive multinucleated cells
80
60
40
20
0
$
OPG
#
#



Figure 7